Sensors & Transducers, Vol. 173, Issue 6, June 2014, pp. 210-214

www.sensorsportal.com

Sensors & Transducers

http://www.sensorsportal.com

The Research on the Characteristics of Micro-fabrication Platform Control System

[1] Xuepeng Liu, [2] Dongsheng Zhang, [3] Xiaohong Hao

[1] Zhongshan Polytechnic,
No. 25, Boai No. 7 Road, Zhongshan City, Guangdong Province, 528404, China
[2] Xi'an Jiaotong University,
No. 28, Xianning West Road, Xi'an City, Shanxi Province, 710049, China
[3] University of Electronic Science and Technology of China,
No. 4, Section 2, North Jianshe Road, City Chengdu, 610054, China
[1] Tel.: 086-0760-88306403, fax: 086-0760-88223722
[1] E-mail: lxpzdm@163.com

Received: 26 May 2014 /Accepted: 27 June 2014 /Published: 30 June 2014

Abstract: X-Y two-axis micro-fabrication platform was controlled by double CPU. The interpolation algorithm and system model were discussed. The repositioning accuracy reached 6.21 μm with moving rate of 2000.00 mm/min. The rate decreased to 1000 mm/min, the contour error is 53.3 μm. The position error and contour error existed due to reverse clearance, reverse step blunt, and servo mismatch. The round error is greater with the increase of moving rate. *Copyright © 2014 IFSA Publishing, S. L.*

Keywords: Repositioning accuracy, Round error, Reverse clearance, Reverse step blunt, Servo match.

1. Introduction

An X-Y micro-fabrication platform control system consisted of a double CPU, servo driver, power supplier, encoder etc. [1-8]. The slave CPU was PMAC motion control card by Delta Tau Company, which implemented real-time motor position and speed control. The master CPU handled task such as track algorithm [9-18], graphics display, and dynamic simulation.

2. Hardware and principle

The CPU of IPC and CPU of PMAC are master-slave double CPU structures. The PMAC controlled the X-Y motion, and the IPC managed the system. The control system included control PC, servo drivers, mechanical motion parts and detectors parts.

PMAC motion card was a programmable multi-axis motion card by Delta Tau Company, which utilized DSP56001/56002 to manipulate 1-8 axes. The card performed motion program, PLC program, and multi-task, communicated with main CPU.

Servo driver was an AC servo motor MSMA043A1A by Panasonic. The speed frequency response reached 500 Hz. The AC permanent magnet servo MOTOR was MSMA042A1C, which reached 3000 r/min.

The actuators were made up of AC MOTOR, clutch, ball screw nut pair, the linear rolling guide, X-Y platform. The platform motion stroke was 300×300 mm. AC motor is connected by ball screw.

3. Control System Software

A control software included interpolation module, servo drive module, PLC monitor module, processing program explanation module, data collecting and digital processing module [19-24].

The interpolation module is made up of linear interpolation and circular interpolation etc. Slave CPU supplied PVT motion module in addition. The interpolation program is the following:

```
CLOSE
&1
#1->2000X
#2->2000Y
;
OPEN PROG 1
CLEAR
RAPID X1 Y4
F500
LINEAR Y13
CIRCLE1 X2 Y14 I1 J0
LINEAR X3
CIRCLE1 X4 Y13 I0 J-1
LINEAR Y7
CIRCLE1 X7 Y4 I3 J0
LINEAR X13
CIRCLE1 X14 Y3 I0 J-1
LINEAR Y2
CIRCLE1 X13 Y1 I-1 J0
LINEAR X4
CIRCLE1 X1 Y4 I0 J3
CWELL 100
RAPID X0 Y0
CLOSE
```

The AC driver module utilized PID position loop. The filter is adjusted by hardness, damp to minimize stable error. The P, I, D parameters are set as 30000, 1280, 10000. The speed forward gain is 2560 to minimize following error caused by less damp, and the acceleration gain is 25600 to minimize following error caused by system inertia.

4. System Model

The platform was connected with the AC servo motor through ball screws, and its transfer function is modeled as:

$$G_S = \frac{X_0(S)}{\theta_i(s)} = \frac{\frac{L}{2\pi}K}{J_S{}^2 + C_S + K}, \tag{1}$$

where $\theta_i(s)$ is the input parameter, $X_0(s)$ is the output parameter, Js is the equivalent moment of inertia, C_s is the equivalent viscous damping coefficient, and K is the equivalent stiffness. The model is a 2-order system.

The AC servo driver part included position control unit, speed control unit and servo motor. The AC servo driver model is:

$$G(s) = \frac{K_m}{s(T_m s + 1)}, \tag{2}$$

where K_m is the motor gain and T_m is the time constant. Therefore the feeding system model is:

$$G(s) = \frac{\frac{L}{2\pi} K_V K_m K_D K}{T_m J_s{}^4 + K_3 s^3 + K_2 s^2 + K_1 s + K_0},$$

$$\begin{aligned} K_3 &= T_m C + J + JK_V K_m K_B, \\ K_2 &= T_m K + C + CK_V K_m K_B, \\ K_1 &= (K + KK_V K_m K_B), \\ K_0 &= \frac{L}{2\pi} K_V K_m K_D K \end{aligned} \tag{3}$$

where J is the moment of inertia of shaft, C is the viscous damping coefficient of shaft, m is the mass of moving parts, and K_m is the stiffness of ball screw nut pair.

5. The Analysis of System Precision

The dynamic characteristics and servo precision of feed system are the main characteristics.

The whole system is simplified as follows (see Fig. 1).

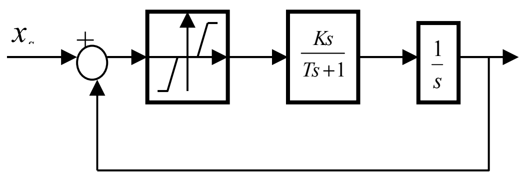

Fig. 1. System model.

where T is the system time constant, K is the servo regulation parameter. The system is I-type system. The stable error is 0 with step input; the stable error is V / K_s with ramp input.

P^* is the expected position vector; P is the real position vector; P_1^* is the position vector closest to P. the contour error vector is defined as:

$$E_r = P_1^* - P = \begin{bmatrix} P_{1x}{}^* \\ P_{1y}{}^* \end{bmatrix} - \begin{bmatrix} P_x \\ P_y \end{bmatrix}, \tag{4}$$

The motion axis had track speed. Therefore E is defined as:

$$E=\begin{bmatrix}E_x\\E_y\end{bmatrix}=P^*-P=\begin{bmatrix}P_x^*\\P_y^*\end{bmatrix}-\begin{bmatrix}P_x\\P_y\end{bmatrix}, \qquad (5)$$

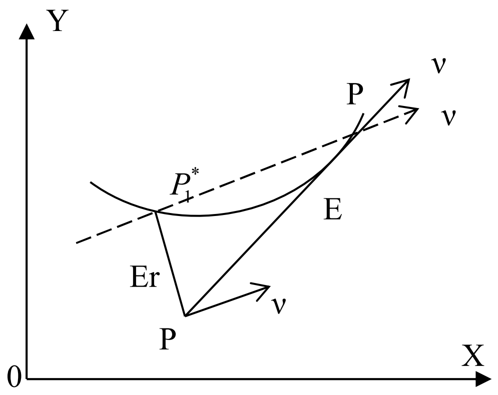

Fig. 2. Curve contour.

The error is deduced:

$$e_r=\left|E_r\right|=\frac{\left|E_xV_y-E_yV_x\right|}{\sqrt{V_x^2+V_y^2}}, \qquad (6)$$

where θ is the intersection angle between P^* tangent and X-axis.

$$\sin\theta=\frac{V_y}{\sqrt{V_x^2+V_y^2}}, \quad \cos\theta=\frac{V_x}{\sqrt{V_x^2+V_y^2}} \qquad (7)$$

Therefore the error is:

$$e_r=E_x\sin\theta-E_y\cos\theta, \qquad (8)$$

The contour error depended on position error $\left(E_x,E_y\right)^T$ and track speed $\left(V_x,V_y\right)^T$. K_{vx} and K_{vy} are X, Y speed error coefficients respectively. The stable errors are:

$$E_x=K_{vx}V_x, \; E_x=K_{vx}V_x \qquad (9)$$

Hence:

$$\varepsilon_r=\frac{V_xV_y}{\sqrt{V_x^2+V_y^2}}\left|K_{vx}-K_{vy}\right|, \qquad (10)$$

The X-axis and Y-axis transfer functions are:

$$\frac{X_0(s)}{X_i(s)}=\frac{\frac{K_x}{\tau_x}}{s^2+\frac{s}{\tau_x}+\frac{K_x}{\tau_x}}, \quad \frac{Y_0(s)}{Y_i(s)}=\frac{\frac{K_y}{\tau_y}}{s^2+\frac{s}{\tau_y}+\frac{K_y}{\tau_y}} \qquad (11)$$

$$\omega_{nx}=\sqrt{\frac{K_x}{\tau_x}}, \quad \omega_{ny}=\sqrt{\frac{K_y}{\tau_y}}, \quad \xi_x=\frac{1}{2\sqrt{K_x\tau_x}}, \quad \xi_y=\frac{1}{2\sqrt{K_y\tau_y}} \qquad (12)$$

The linear error is:

$$e_{ss}(t)=\frac{V\sin2\theta}{2}\left(\frac{1}{K_y}-\frac{1}{K_x}\right), \qquad (13)$$

The static linear contour error is 0 when $2\theta=0$. The error is maximum when $\theta=45$. The error is:

$$e_{ss}(t)=\frac{V}{2}\left(\frac{1}{K_y}-\frac{1}{K_x}\right), \qquad (14)$$

The static linear contour error is 0 as 2-axis dynamic characteristics matched.

The circular static error is:

$$\frac{e_r}{R}=1-\frac{1}{\sqrt{1+2(\frac{\omega}{\omega_n})^2+(\frac{\omega}{\omega_n})^4+(\frac{2\xi\omega}{\omega_n})^2}}, \qquad (15)$$

6. Experiments

In Fig. 3 curve 1 shows the ideal contour while curve 2 shows the real contour. Curve 1 is round since x axis and y axis dynamic characteristics matched well. The static contour error became larger in curve 2 while the dynamic characteristics mismatched.

Position precision and repositioning accuracy were detected when there was not loaded. Six point data were chosen, and each point data was measured seven times to calculate average value and scatter errors ±3Sj. The whole data are showed in Table 1. The repositioning accuracy reached 6.21 μm

($A=(X_j+3S_j)_{\max}-(X_j-3S_j)_{\min}$) with moving rate of 2000.00 *mm/min*. the position precision reached 6 *μm*.

The real contour was ellipse when machine made a round motion.

The Renishaw QC10 ball bar instrument was utilized to measure round error, and the measuring radius was 150.00 mm. The following figures showed round errors at rate of 1000.00 mm/min and 2000.00 mm/min.

When the feedrate is 2000 mm/min, the contour error is 83.3 *μm*. The rate decreased to 1000 mm/min, the contour error is 53.3 *μm*. When the feedrate decreased, the interpolation precision increased and the system precision increased.

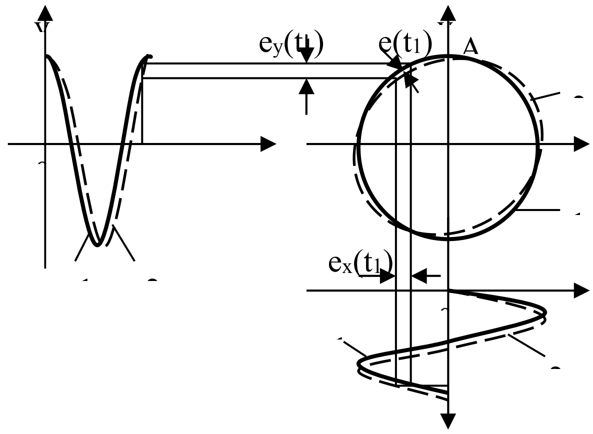

Fig. 3. Contour error.

Table 1. Position precision.

Position number		**1**	**2**	**3**	**4**	**5**	**6**
Position		25.485	72.610	147.725	196.445	242.560	283.385
Deviation (μm)	1	0.5	1	1	2.5	5	6
	2	1	0.8	1	4.5	6	5.5
	3	1	0.5	0	2	5	5.5
	4	0.5	1	2	2.5	5	3.5
	5	0.6	-0.2	1	3.0	5	4
	6	1	0.7	1	3.0	4.5	3.5
	7	1	0.7	1	2.8	5.2	5
Mean deviation Xj		0.8	0.7	1	2.9	5.1	4.7
Standard deviation Sj		0.252	0.416	0.577	0.787	0.451	1.035
Max deviationMj		1	1	2	4.5	6	6
3Sj		0.755	1.249	1.732	2.362	1.353	3.105
Xj+3Sj		1.555	1.949	2.732	5.262	6.453	7.820
Xj -3Sj		0.045	-0.549	-0.732	0.538	3.747	1.609

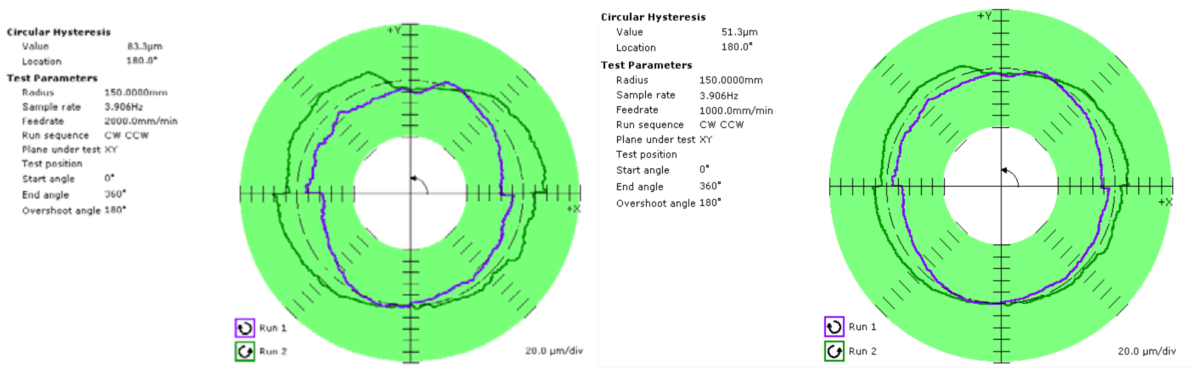

Fig. 4. Contour curve at feedrate of 1000.00 mm/min and 2000 mm/min.

6. Conclusion

There were reverse clearance, reverse step blunt, and servo mismatch, which resulted in position errors and ellipse track.

The reverse clearance is classified as positive, negative and un-equivalent value. The system clearance is un-equivalent value which showed different reverse clearance in double direction. The reasons were as follows:

1) There was clearance between drivers system;

2) The end of ball screw was floating;

3) The screw was reversed for over larger preload;

4) There are clearance or floating between rolling guide.

The reverse step blunt was small peak in Fig. 4 in X-axis. The reasons were as follows:

1) The torque was not enough, thus caused viscous pause at the direction-changing point.

2) The servo response time was incorrect at reverse clearance compensation, which didn't compensate in time. Therefore the shaft paused.

3) The servo response was insensitive between the direction and changing point, which caused delay between shaft changing directions.

The figure was ellipse at servo mismatch.

The servo loop gain mismatch at different shaft which caused servo mismatch, therefore one shaft advanced before the other. The advanced shaft had a large gain.

Moreover, different feed rate had an influence on contour. The larger was the feed rate, the larger was round error. The Fig. 4 demonstrated the phenomena.

Acknowledgements

The work is supported by National Science and Technology Major Project (2012ZX04012032).

References

[1]. Liu Huran, Computer aided simulation machining programming in 5-Axis Nc milling of impeller leaf, *Physics Procedia*, Vol. 25, 2012, pp. 1457-1462.

[2]. Zhixiang Shao, Ruifeng Guo, Jie Li, Accurate modeling method for generalized tool swept volume in 5-axis NC machining simulation, *Journal of Software*, Vol. 6, No. 10, 2011, pp. 2056-2063.

[3]. Bo Zhou, Jibin Zhao, Weijun Liu, Generation method for five-axis NC spiral tool path based on parametric surface mapping, *Journal of Systems Science and Complexity*, Vol. 26, Issue 5, 2013, pp. 676-694.

[4]. Liu Hang, Liu Meiyu, Tool path planning for high speed milling of sculpture surface with toroidal cutter, *Modeling and Simulation*, Vol. 2, Issue 3, 2013, pp. 27-30.

[5]. R. Shabani, S. Tariverdilo, H. Salarieh, Nonlinear identification of electro-magnetic force model, *Journal of Zhejiang University Science A*, Vol. 11, No. 3, 2010, pp. 165-174.

[6]. Yoshiyuki Tomita, Yasushi Koyanagawa, Fumiaki Satoh, A surface motor-driven precise positioning system, *Precision Engineering*, Vol. 16, 3, 1994, pp.184-191.

[7]. Rong-Fong Fung,Yi-Lung Hsu, Ming-Shyan Huang System identification of a dual-stage XY precision positioning table, *Precision Engineering*, Vol. 33, 1, 2009, pp.71-80.

[8]. Chien-Hung Liua, Wen-Yuh Jyweb, etc, Design and control of a long-traveling nano-positioning stage, *Precision Engineering*, Vol. 34, 3, 2010, pp.497-506.

[9]. S. Verma, W. J. Kim, J. Gu, Six-axis nanopositioning device with precision magnetic levitation technology, *IEEE/ASME Transactions on Mechatronics*, Vol. 9, Issue 2, 2004, pp. 384-391.

[10]. Zhang Yi, Ma Shu-Yuan, Sun Hui-Zhi, et al, Nonlinear control of magnetic jiggle stage based on differential geometry method, *Nanotechnology and Precision Engineering*, Vol. 9, No. 3, 2011, pp. 244-248.

[11]. Liu Xuepeng, Mei Xuesong Wu Xutang, A 2-order positioning system of surface-motor, *China Mechanical Engineering*, Vol. 15, No. 13, 2004, pp. 1176-1178.

[12]. Zhao Xing-Yu, Zhang Sheng-Quan, Zhang Da-Wei, Design and simulation of the control system of precision positioning table driven by voice coil actuator, *Journal of Tianjin University,* Vol. 40, No. 2, 2007, pp. 127-132.

[13]. Isao Satou, Development of advanced silylation process for 157-nm lithography, *Microelectronic Engineering*, Vol. 3, 2001, pp. 571-577.

[14]. J. W. Jansen, C. M. M. Lierop, E. A. Lomonova, et al, Modeling of magnetically levitated planar actuators with moving magnets, *IEEE Transactions on Magnetics,* Vol. 43, Issue 1, 2007, pp. 15-25.

[15]. Lars Monch, Matthias Prause, Simulation-based solution of load-balancing problems in the photolithography area of a semiconductor wafer fabrication facility, in *Proceedings of the Winter Simulation Conference*, 2001, Vol. 2, pp. 1170-1177.

[16]. Valery M. Dubin, Electrochemical aspects of new materials and technologies in microelectronics, *Microelectronic Engineering*, Vol. 70, Issue 2, 2003, pp. 461-469.

[17]. Cao Jiayong, Zhu Yu, Wang Jinsong, et. Al, A novel synchronous permanent magnet planar motor and its model for control applications, *IEEE Transactions on Magnetics*, Vol. 41, Issue 6, 2005, pp. 2156-2163.

[18]. Liu Xue-Peng, Hao Xiao-Hong, Zhang Hong-Ding, Ma Teng, Modeling and control for analog inner loop and digital outer loop of nanotechnology-stage in X-Y direction, *Microfabrication Technology*, Vol. 4, 2003, pp. 73-77.

[19]. X. M. Shan, S. K. Kuo, J. Zhang, C. H. Menq, Ultra precision motion control of a multiple degrees of freedom magnetic suspension stage, *IEEE/ASME Transactions on Mechatronics*, Vol. 7, Issue 1, 2002, pp. 67-78.

[20]. H. Yu, and W. J. Kim, A compact hall-effect-sensing 6-DOF precision positioned, *IEEE Transactions on Control Systems Technology*, Vol. 15, Issue 6, 2010, pp. 982−985.

[21]. J. C. Compter, Electro-dynamic planar motor, *Precision Engineering*, Vol. 28, No. 2, 2004, pp. 171-180.

[22]. M. Gajdusek, J. de Boeij, A. H. Damen, et al, Contactless planar actuator with manipulator – Experimental setup for control, in *Proceedings of the 6th International Symposium on Linear Drives for Industry Applications (LDIA'2007),* Lille, France, 16-19 September 2007.

[23]. S. J. Kwang, S. B. Yoon, Contact-less revolving stage using transverse flux induction principle, *Precision Engineering*, Vol. 33, Issue 1, 2009, pp. 107-115.

[24]. Zhang Dongsheng, Mei Xuesong, Hao Xiaohong et al, Modeling dynamic magnetic force and robust control, in *Proceedings of the 16th IEEE International Conference on Control Applications*, 2007, 349-354.